Available online at www.sciencedirect.com
SCIENCE DIRECT®
Journal of Chromatography B, 808 (2004) 279–286
JOURNAL OF CHROMATOGRAPHY B
www.elsevier.com/locate/chromb

Proteomic analysis of an orthotopic neuroblastoma xenograft animal model☆

Natascia Campostrini[a], Jennifer Pascali[a], Mahmoud Hamdan[b], Hubert Astner[a], Danilo Marimpietri[c], Fabio Pastorino[c], Mirco Ponzoni[c], Pier Giorgio Righetti[a,*]

[a] *Department of Agricultural and Industrial Biotechnologies, University of Verona, Strada le Grazie 15, 37134 Verona, Italy*
[b] *Computational, Analytical and Structural Sciences, GlaxoSmithKline, Via Fleming 4, 37135 Verona, Italy*
[c] *Laboratory of Oncology, G. Gaslini Children's Hospital, Genoa, Italy*

Received 16 March 2004; received in revised form 4 May 2004; accepted 17 May 2004

Available online 17 June 2004

Abstract

Neuroblastoma is the most common extracranial solid tumour of childhood and comprises up to 50% of malignancies among infants. There is a great need of designing novel therapeutic strategies and proteome analysis is one approach for defining markers useful for tumour diagnosis, as well as molecular targets for novel experimental therapies. We started by comparing healthy adrenal glands (which are the election organs developing primary neuroblastoma, NB, tumours) and adrenal glands carrying primary NB tumours, taken from nude mice. Standard maps of healthy and tumour samples were generated by analysis with the PDQuest software. The comparison between such maps showed up- and down-regulation of 84 polypeptide chains, out of a total of 700 spots detected by a fluorescent stain, Sypro Ruby. Spots that were differentially expressed between the two groups, were analysed by MALDI-TOF mass spectrometry and 14 of these spots were identified so far. Among these proteins, of particular interest are the down-regulated proteins adrenodoxin (21-folds), carbonic anhydrase III (eight-folds) and aldose reductase related protein I (eight-folds), as well as the up-regulated protein peptidyl-propyl *cis–trans* isomerase A (five-folds). Moreover new proteins, which were absent in control samples, were expressed in tumour samples, such as nucleophosmin (NPM) and stathmin (oncoprotein 18).

Keywords: Proteomics; Neuroblastoma; Two-dimensional maps

1. Introduction

Neuroblastoma (NB), together with lymphoma, osteosarcoma, Ewing's tumours, rhabdomyosarcoma and lymphoblastic leukemia, belongs to a group of undifferentiated paediatric malignancies known as the small round-cell tumours of childhood. NB is the most common extracranial solid tumour of infancy and childhood. It arises from primitive neuroepithelial cells of the neural crest and occurs in the adrenal medulla or paraspinal symphatetic ganglia of the abdomen, chest or neck [1]. NB accounts for approximately 9% of all childhood cancers, occurring once out of 8000 live births. This results in an annual incidence of approximately one in 100,000 children less than 15 years of age world-wide. The median age at diagnosis is approximately 22 months with over one-third diagnosed at less than 1 year and over 88% diagnosed by the age of 5.

Despite various therapeutical treatments, including radio-, immune- and chemio-therapy, at elevated doses, with or without bone marrow transplant, childhood cancers caused by neural crest cells, are still characterised by a high percentage of relapse and a high rate of mortality. Starting from these considerations, there is a great need for designing novel therapeutic strategies. The effective treatment of NB, either at advanced stages or at minimal residual disease, remains one of the major challenges in paediatric oncology.

Abbreviations: NB, neuroblastoma; NPM, nucleophosmin; MALDI-TOF, matrix assisted laser desorption/ionisation time of flight

☆ Presented at the 3rd Meeting of the Spanish Association of Chromatography and Related Techniques and the European Workshop, 3rd Waste Water Cluster, Aguadulce (Almeria), 19–21 November 2003.

* Corresponding author. Tel.: +39 045 8027901; fax: +39 045 8027929.
E-mail address: righetti@sci.univr.it (P.G. Righetti).

1570-0232/$ – see front matter © 2004 Elsevier B.V. All rights reserved.
doi:10.1016/j.jchromb.2004.05.013

Prognosis for patients with this disease has improved with advances in medical care but the overall 5 year survival is still less than 60% [2]. Indeed, the incidence of fatal relapses is still high and long-term survival remains very low [3]. Innovative therapies are thus required and should be focused on the genes and biological pathways that might contribute to malignant transformation or progression of this neoplasia.

To be highly effective, cancer therapy has to be individualised. This requires a detailed understanding of the properties of each tumour with regard to metastasising propensity and drug sensitivity, information that is difficult or even impossible to gain from microscopic analysis of hematoxylin-stained tissue sections. Detailed information regarding mutations in growth-controlling genes, expression of genes controlling growth, metastasis and drug resistance must be obtained. Proteome analysis today, is perhaps one of the most valuable tools for defining markers useful for tumour diagnosis [4]. In addition, proteomics has the potential to unravel basic tumour biological questions regarding mechanisms involved in the pathogenesis of cancer. In this study, we present a first proteomic approach to NB analysis, based on an orthotopic neuroblastoma animal model.

2. Materials and methods

2.1. Chemicals and materials

Tris, mineral oil, DL-dithiothreitol (DTT), Tween 20 and EDTA were purchased from Sigma–Aldrich Chemie Gmbh (Steinheim, Germany). Glycerol, methanol, ethanol, acetic acid and acetone were from Merck (Darmstadt, Germany). Forty percent acrylamide/Bis solution, *N*,*N*,*N*′,*N*′-tetramethylethylene diamine (TEMED), acrylamide, ammonium persulfate (APS), the Protean IEF Cell, the GS-710 Densitometer, the Versa Doc Scanner, the software PDQuest Version 6.2 as well as the linear Immobiline dry strips pH gradient 3–10 (17 and 7 cm long), pH gradient 4–7 (7 cm long) were obtained from Bio-Rad Labs (Hercules, CA, USA); glycine, sodium dodecyl sulphate (SDS), iodoacetamide, urea, thiourea, tributylphosphine (TBP) and CHAPS were from Fluka. Bromophenol blue, carrier ampholytes and agarose were purchased from Pharmacia Biotech (Uppsala, Sweden).

2.2. Orthotopic neuroblastoma animal model

Five-week-old female nude (nu/nu) mice were purchased from Harlan Laboratories (Harlan Italy-S. Pietro al Natisone, UD). Mice were anaesthetised and injected with 5×10^4 cultured murine NXS2 neuroblastoma cells [5] (kindly provided by Dr. Reisfield, Scripps Clinic, La Jolla, CA, USA) in 20 μL of HEPES buffer, after laparatomy, in the capsule of the left adrenal gland. The lethality of the method was 0%. Mice were monitored at least two times weekly for evidence of tumour development, quantification of tumour size, and evidence of tumour-associated morbidity. Mice were sacrificed and organs, after washing in PBS, were frozen and stored in liquid nitrogen. All experiments involving animals have been reviewed and approved by the licensing and ethical committee of the National Cancer Research Institute and by the Italian Ministry of Health.

Four samples, divided in two classes, constituted the dataset:

- Four samples from healthy adrenal nude mouse glands (the pool of which was used to perform four 2D-maps; Fig. 1a);
- Four samples from adrenal nude mouse glands carrying primary Neuroblastoma tumours (the pool of which was used to perform four 2D-maps; Fig. 1b).

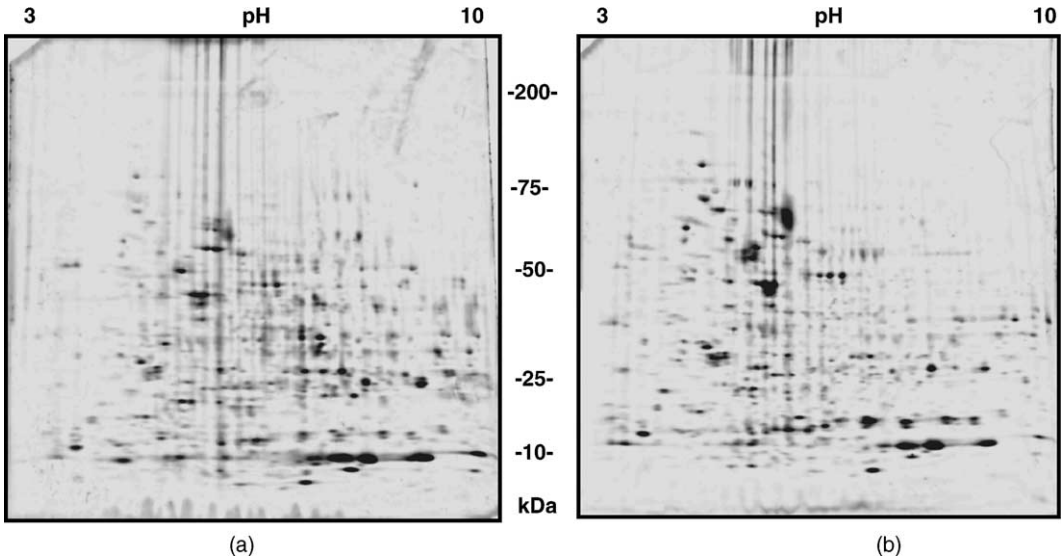

Fig. 1. Examples of the obtained 2D-PAGE maps: control (a) and tumour (b) samples.

The procedure was repeated three times, thus producing three genuine replicates for each map.

2.3. Two-dimensional gel electrophoresis

2.3.1. Sample treatment

Healthy and tumour adrenal glands from nude mice were stored at −80 °C. All samples were homogenised (5% homogenate) with a lysis solution containing 7 M urea, 2 M thiourea, 3% CHAPS, 40 mM Tris, 5 mM TBP, 0.5% carrier ampholytes pH 3–10, 5 mM EDTA, 1 mM PMSF and 50 U/mL DNAse. After 1 h lysis, samples were centrifuged at 4 °C at 6000 rpm for eliminating all residual particles. The collected supernatant was alkylated for 1 h with 10 mM acrylamide (1 M stock solution) and the reaction was stopped with 10 mM DTT (from 1 M stock solution) [6]. Interfering substances (lipids, salts) were removed by a precipitation step. A cold mix of acetone and methanol (8:1) was added; after 2 h at −20 °C, the solution was centrifuged at 13,000 rpm for 30 min. Pellets were finally resuspended in sample solution containing urea, thiourea, CHAPS and Tris.

2.3.2. IEF in IPG strips

The first dimension run was performed on strips (17 cm length, 0.5 mm thickness) with a linear pH gradient from pH 3 to 10 [7]. The IPG strips were rehydrated with 400 μg of pooled samples (four strips with pooled healthy samples and four strips with pooled tumour samples) and containing traces of bromophenol blue for monitoring the electrophoretic run. The passive gel rehydration was allowed to continue for 8 h before the focusing step. Isoelectric focusing (IEF) was carried out with a Protean IEF Cell (Bio-Rad), with a low initial voltage and then by applying a voltage gradient up to 10,000 V with a limiting current of 50 μA/strip. The total product time × voltage applied was 75,000 Vh for each strip and the temperature was set at 20 °C.

2.3.3. Interfacing the IPG strips with the denaturing SDS solution and SDS–PAGE

Each strip was equilibrated with a SDS denaturing solution containing 6 M urea, 2% SDS, 20% glycerol, 0.375 M Tris–HCl (pH 8.8). The contact lasted for 30 min in tubes containing 20 mL each of the equilibration solution. Each strip was then interfaced with a gel slab using 0.5% agarose solubilised in the cathodic buffer (192 mM glycine, 0.1% SDS, Tris to pH 8.3). All the gel slabs were cast with a two-vessel gradient mixer, with total sufficient volumes for polymerising eight gel slabs of 1.5 mm in thickness and with a porosity gradient from 7 to 20%T. Polymerization took place overnight. The second dimension run was performed by using a PROTEAN II xl Multi-Cell (Bio-Rad). The cathodic buffer was the same as in previous step; the anodic buffer was a solution of 0.375 M Tris–HCl, pH 8.8. The electrophoretic run was performed by setting a current of 2 mA for each gel for 1 h, then 5 mA/gel for 2 h and 10 mA/gel until the end of the run. During the whole run the temperature was set at 11 °C.

2.4. Fluorescent staining

All gels were fixed with a solution containing 40% ethanol and 10% acetic acid for 30 min. After this step the gels were stained with Sypro Ruby (70 mL for each gel) overnight and then destained with 10% methanol, 7% acetic acid for 1 h. The gels were finally washed with milliQ water. All the samples were then digitised with the Versa Doc Scanner.

2.5. Protein pattern and statistical analysis

The digitised images were acquired with the software PDQuest (version 6.2), which was used for cropping and orienting the images, for detecting and identifying spots, for comparing and matching spots, for normalising and analysing the data and for preparing a report. A match set was created from the protein patterns of the two independent cellular extracts (healthy mouse adrenal gland, mouse adrenal gland carrying NB primary tumours). A standard gel was generated out of the image with the highest spot number. Spot quantities of all gels were normalised by removing non expression-related variations in spot intensity; for that, the raw quantity of each spot in a gel was divided by the total quantity of all the spots in that gel and included in the standard. The final synthetic image was a Gaussian scan image that contained all the Gaussian spots with a defined volume and quality. All subsequent spot matching and analysis steps in the PDQuest software were performed on Gaussian spots. The results were evaluated in terms of spot optical density (OD). Statistical analysis (Student's *t*-test) via PDQuest allowed the study of proteins that were significantly increased or decreased in pathological samples.

2.6. Protein identification by mass spectrometry

2.6.1. In situ digestion and extraction of peptides and MALDI-TOF analysis

The spots of interest were carefully excised from the gel with a razor blade and placed in Eppendorf tubes. The gel pieces were washed twice with a solution of acetonitrile/Tris 5 mM pH 8.5 (50/50) followed by a single wash with only Tris 5 mM pH 8.5. These pieces were dehydrated in Speedvac device at room temperature and covered with 15 μL of Trypsin (0.02 mg/mL) in NH_4HCO_3 buffer (40 mM, pH 8.5) and left at 37 °C overnight. The peptides were extracted two times in 50 μL of acetonitrile/H_2O 1% (v/v) formic acid (50/50). The extraction was conducted in an ultrasonic bath for 15 min each time. After sonication, the excess of acetonitrile was evaporated and the peptides were resuspended in 10 μL of 0.1% TFA, concentrated and cleaned using ZipTip microcolumns (C18).

The extracted peptides were loaded onto the MALDI target plate by mixing 1 μL of each solution with the same

volume of a matrix solution, prepared fresh every day by dissolving 10 mg/mL cyano-4-hydroxycinnamic acid in acetonitrile/ethanol (1:1, v/v), and allowed to dry. Measurements were performed using a TofSpec 2E MALDI-TOF instrument (Micromass, Manchester, UK), operated in the reflectron mode, with an accelerating voltage of 20 kV [8]. The laser wavelength was 337 nm and the laser repetition rate was 4 Hz. The final mass spectra were produced by averaging 50–200 laser shots. Peptide masses were searched against SWISS-PROT, TrEMBLE and NCBInr databases by utilizing the ProteinLynx program from Micromass, Profound from Prowl and Mascot from Matrix Science.

2.7. Immunoblot analysis

Proteins derived from healthy and tumour adrenal glands, previously separated by 2D-PAGE, were transferred onto PVDF membranes (Immuno-Blot™ PVDF membrane, Bio-Rad) for 2 h at 60 V, using a Mini Trans-Blot system (Bio-Rad). Membranes were blocked with 3% BSA in TBST (10 mM Tris, 150 mM NaCl, 0.1% Tween 20, pH 7.5) overnight at 4 °C and then incubated for 1 h at room temperature with the anti-OP18/stathmin antibody (1:5000, Sigma), recognising the C-terminus of this protein. Blots were developed with an enhanced chemiluminescence system (ECL plus, Amersham) and stathmin visualised on an autoradiography film (Hyperfilm, Amersham). Films were scanned using a densitometer (GS-710, Bio-Rad).

3. Results and discussion

3.1. Biological relevance of the orthotopic neuroblastoma xenograft model

Previous in vivo experiments, by using directly an i.v. administration of NB cells in nude mice, have proved the importance of choosing a specific xenograft animal model that mimics the metastatic spread observed in advanced-stage human NB patients [9,10]. However, a further and more realistic view of a comparative study could be obtained if a tumour model were available that better reflected the growth of advanced NB in children (i.e. large adrenal gland tumours and multiple small metastatic lesions). All current data support this concept and recommend that orthotopic implantation of tumour cells in recipient animals is mandatory for

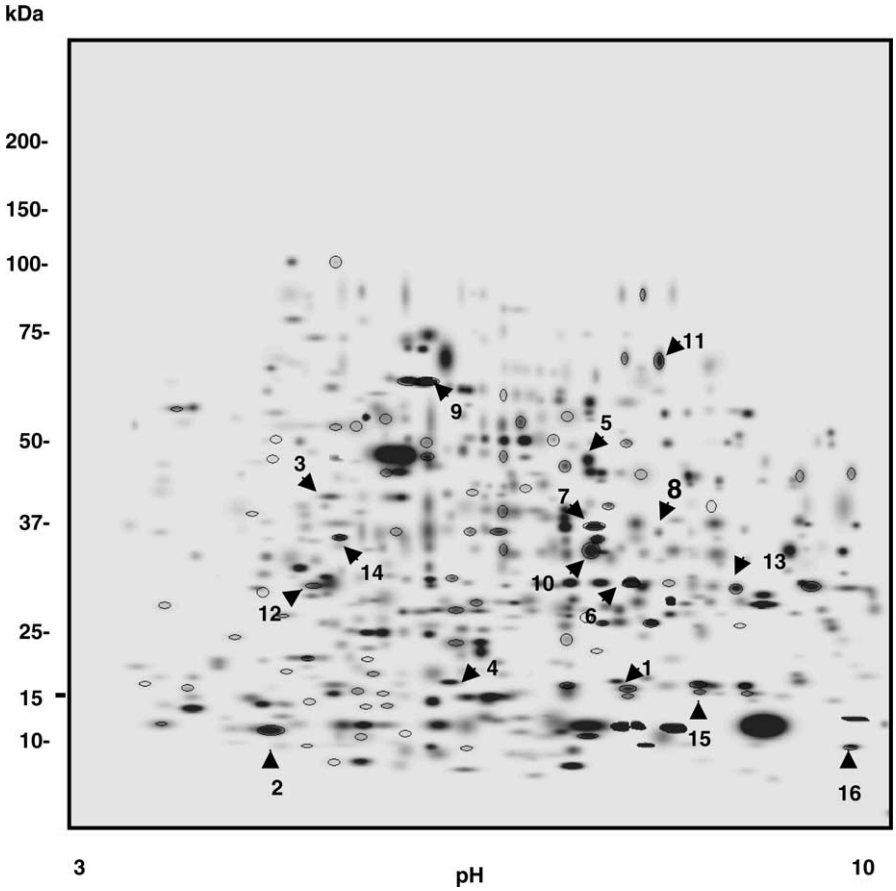

Fig. 2. Master map of a neuroblastoma tissue excised from the adrenal glands of nude mice. The 84 spots differently expressed are circled and the identified spots are numbered. The circled numbered spots refer to the 14 spots which could be identified by mass spectrometry upon excision (two of them, spots 15 and 16, gave good spectra but could not be found in any of the data bases available).

studies of tumour progression, angiogenesis, invasion, and metastasis [11]. In order to provide a well characterised, relevant, highly reproducible, angiogenic, and metastatic orthotopic model of NB, we initiated studies to define an adrenal NB xenograft model. We decided to use the intra-adrenal injection of NXS2 murine NB cells in mice because, 2 weeks after injection, adrenal gland tumours were always found in all animals. This model best reflected the typical growth pattern of human NB, since orthotopic injection of NXS2 cells resulted in solid adrenal tumours that were highly vascular, locally invasive into surrounding tissues, and metastatic to distant sites. Indeed, macroscopic metastases always occurred after 3–4 weeks of injection in the ovary and spleen, while micrometastases were apparent frequently in the contralateral adrenal gland, kidneys, liver, bone marrow and lung.

3.2. 2D map analysis

Fig. 2 shows the master map of the neuroblastoma developed in nude mice: about 750 spots could be counted upon Sypro Ruby staining. They seem to be quite evenly distributed in the pH 3–10 interval, with a Mr distribution from ca. 9000 to 140,000 Da. The circles mark 84 spots found to be differently expressed in pathological samples, of which 39 were up-regulated and 45 down-regulated. Moreover, a number of protein spots that were newly expressed and newly silenced in the tumour samples as compared to healthy ones could also be detected. Additionally, the numbers refer to the 14 spots which could be identified by MS analysis (an additional two, numbers 15 and 16, although producing good quality spectra, could not be matched to any of the databases available). Fig. 3 shows a small gel area with a few spots up- and down-regulated and newly expressed in pathological versus control specimens. Table 1 lists the protein spots that could be identified so far. In general, there was a good agreement between the theoretically-predicted and experimentally found p*I* and Mr values, except for a large deviation in the case of adrenodoxin, suggesting that this protein might be extensively modified at the post-translational level in this kind of tissue, or be a pre-protein, as discussed below. Adrenodoxin, in fact, (ADX) is a small iron–sulfur protein present in the mitochondrial matrix, where it transfers electrons from adrenodoxin reductase to mitochondrial forms of cytochrome *P*-450. The adrenal cortex is one of the more abundant sources of adrenodoxin, since it interacts with the three mitochondrial, steroidogenic *P*-450s. Adrenodoxin is also expressed in other steroidogenic tissues such as testis, ovary and placenta as well as in nonsteroidogenic tissues where mitochondrial *P*-450 forms are active including liver, kidney and brain. Adrenodoxin is encoded as larger precursors of 188 amino acids, and the signal peptide is cleaved during transfer into mitochondria (64 amino acids). The M_r of the mature adrenodoxin chain (124 amino acids) is 13,617 Da: this is in agreement with our experimental data. The mouse adrenodoxin pre-protein is 93, 74, 70 and

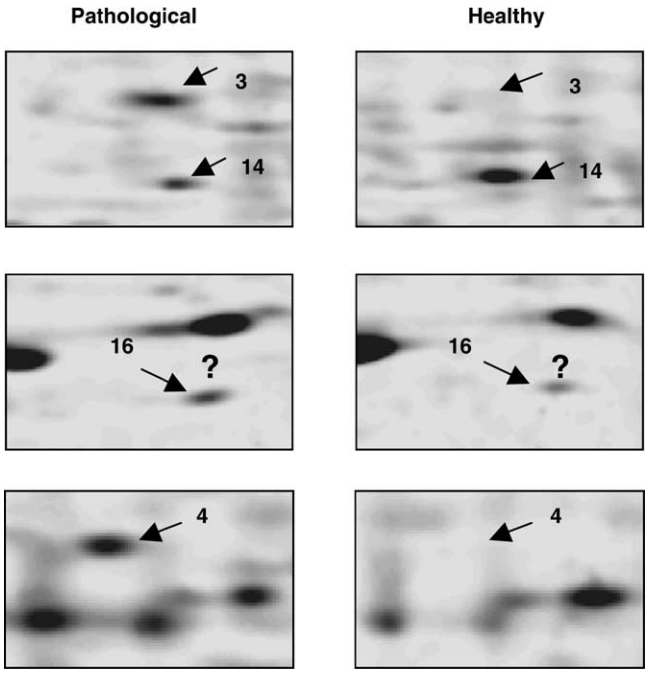

Fig. 3. Comparison of two-dimensional gel patterns of some proteins in neuroblastoma (left panel) and healthy (right panel) tissues. The corresponding spot number are shown in Table 1. The spot with a question mark corresponds to a two-fold up-regulated protein which could not be identified in any of the databases available, although it gave good MS spectra.

69% identical to the rat, human, bovine and porcine adrenodoxin pre-proteins, respectively. The mature adrenodoxin is 98% identical to rat adrenodoxin and 90% identical to the human, bovine and porcine adrenodoxin [12].

In order to further confirm the data obtained with the master map, we performed an immunoblot analysis on stathmin, a protein which, together with nucleophosmin (NPM), appears to be expressed only on tumour samples (Fig. 3). As shown in Fig. 4, with this method low levels of this stathmin can also be detected in normal murine tissue (right panel), whereas in the tumour sample (left panel) the same spot appears to be over-expressed by a factor of at least >15 times. Additionally, when the same experiment was repeated in a shallower pH gradient (pH 4–7) this very intense spot (which appeared oblong in the wide pH range) could be resolved into a well-separated string of minor spots, more acidic than the parental protein. This experiment suggests two important points, which might have escaped detection up to the present. First of all, it might not be true that a gene is fully silenced or newly turned-on in pathological tissues (or during ontogenesis or any other biologically-relevant phenomenon, such as differentiation, cell-cycle arrest, apoptosis, cell modification induced by drug treatments) as compared to the control, healthy one. Indeed, extremely low levels might be present in the control samples, and vice versa. What our experiments suggest is that, in the control samples, the levels of stathmin were so minute as to be below the sensitivity limit of Sypro Ruby staining. With immuno-detection (the most

Table 1
Identified proteins from the neuroblastoma tissue

	Experimental Mr (Da)	Experimental p*I*	Theoretical Mr	Theoretical p*I*	Z-score	MOWSE-score	Protein name	Accession number	Coverage (%)	Number of peptides	Variation
1	∼15000	7.8	17,840	8.3	2.39	1.93E8	Peptidyl-prolyl *cis–trans* isomeraseA	P17742	59.5	13	Increased 5
2	∼13000	5.0	20,123	5.5	1.84	1.60E4	Adrenodoxin	P46656	25	8	Decreased 21
3	∼40000	4.5	32,560	4.6	2.38	2.51E5	Nucleophosmin (NPM)	Q61937	31	8	Only tumoral samples
4	∼17000	6.5	17,143	6.0	2.33	3.78E7	Stathmin (OP18)	P54227	64.9	17	Only tumoral samples
5	∼50000	7.5	46,661	6.9	2.31	4.46E8	Isocitrate dehydrogenase	O88844	33.3	15	Only control samples
6	∼30000	7.8	29,366	7.4	1.67	1.78E5	Carbonic anhydrase III	P14141	28	8	Decreased 8
7	∼37000	7.5	35,857	7.2	2.29	1.77E11	Aldose reductase related protein1	P21300	59.3	18	Decreased 8
8	∼35000	8.0	33,335	8.2	2.1	2.68E7	Thiosulfate sulfurtransferase	P52196	39	13	Only control samples
9	∼65000	6.5	60,956	6.1	2.37	2.61E21	60 kDa heat shock protein	P19226	57	37	Decreased 4
10	∼34000	7.5	34,973	8.6	2.38		Electron tranfer flavoprotein	NCBI gi21704230	41	12	Decreased 4
11	∼72000	8.1	67,631	7.7	2.41	2.09E9	Transketolase	P40142	28	18	Decreased 2
12	∼30000	5.1	27,771	4.8	2.06	2.57E6	14-3-3 protein zeta/delta (protein kinase C inhibitor protein-1)	P35215	42	9	Increased 2
13	∼27000	8.9	31,517	8.6	2.28	6.78E6	Enoyl-CoA hydrase	P14604	34	10	Decreased 4
14	∼36000	5.3	35,753	4.8	2.38	2.70E13	Annexin V	P48036	64	22	Decreased 2
15	∼15000	8.5	?	?	?	?	?	?	?	?	Increased 3
16	∼8500	9.8	?	?	?	?	?	?	?	?	Increased 2

The comparison is performed between the matched spots in healthy samples and the matched spots in tumoural ones. A threshold value of 2.0 (which corresponds to a variation of 100%) was chosen as a meaningful variation in the comparison of tumour proteins vs. healthy proteins. The number, written in the last column, means folds of change.

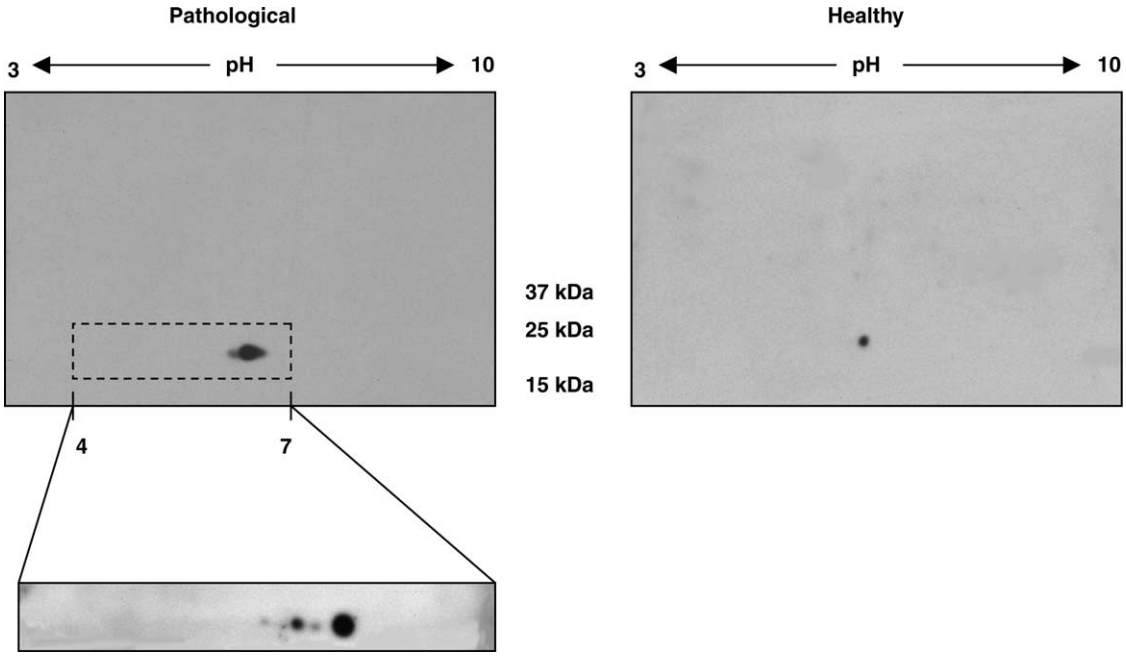

Fig. 4. Immunoblots of 2D-PAGE slabs from normal murine samples (right panel) and tumour tissues (left panel), developed by using an anti-OP18/stathmin antibody, recognising the C-terminus of this protein. Lower strip on the left: same boxed area of the upper gel, but run in a shallower (pH 4–7) IPG gradient. Note the string of spots to the left of the parental spot, suggesting a phosphorylated train.

sensitive detection method today available) detectable levels of stathmin could indeed be found also in control tissue (Sypro Ruby has a sensitivity at least three orders of magnitude lower than our chemiluminescence detection method on the immunoblot) [13]. The other very important point, is that only with such a sensitive method we could observe that, in tumour tissues, stathmin seems to be modified, possibly at the post-synthetic level, the p*I* variations in the string of minor spots suggesting that there could be phosphorylation events.

3.3. On the significance of nucleophosmin and stathmin up-regulation

Our group is now extensively involved in the proteomic analysis of different human tumours, such as mantle cell lymphomas [14,15] and pancreatic ductal carcinomas [16]. In both cases we found strong variations of these two proteins, whose significance will be discussed below. Nucleophosmin, a three-fold down-regulated protein, appears to be particularly important in oncogenesis. NPM is a ubiquitously expressed nuclear phosphoprotein that continuously shuttles between the nucleus and cytoplasm. One of its suggested roles is in ribosomal protein assembly and transport and also as a molecular chaperone that prevents proteins from aggregating. Evidence is accumulating that the NPM gene is involved in several tumour-associated chromosome translocations and in the oncogenic conversion of various associated proteins [17–19]. NPM appears to be present in most human tissues, with especially robust expression in pancreas and testis and lowest expression in lung [20]. Interestingly, a fusion protein, containing the amino-terminal 117 amino acid portion of NPM, joined to the entire cytoplasmic portion of the receptor tyrosine kinase anaplastic lymphoma kinase (ALK) has been found to be involved in oncogenesis in the case of non-Hodgkin's lymphoma [21]. Stathmin (oncoprotein 18, OC18) is a p53-regulated member of a novel class of microtubule-destabilising proteins known to promote microtubule depolymerisation during interphase and late mitosis [22–25]. Noteworthy, over-expression of stathmin, by inhibiting polymerisation of microtubules, permits increased binding to these structures of vinblastin, a well known chemotherapeutic agent, during treatment of human breast cancer [22].

4. Concluding remarks

To our knowledge, this is the first attempt, at a proteome level, of analysis of the paediatric solid tumour neuroblastoma. At present, we were forced to adopt a clinically relevant animal model, by injecting murine NB tumour cells in the capsule of the left adrenal gland of nude mice, due to the fact that human studies are hampered by the difficulty to procure proper, healthy controls. Although preliminary in nature, these studies will be quite valuable in view of extending them to human cases. At the Gaslini hospital, in fact, we have a rather large collection of NB tumour biopsies taken after surgery; as soon as control tissues will be available, the present data could be easily extended to human tumours, in view of finding the possible mechanisms, at the proteome, transcriptome and genome levels, responsible for

their development. Future studies will thus be addressed to human cases as well as to the correlation between regulation of protein expression and mRNA levels present in the cells.

Acknowledgements

Supported by grants from Associazione Italiana per la Ricerca sul Cancro (AIRC) and from Fondazione Italiana per la Lotta al Neuroblastoma. PGR is additionally supported by grants from MIUR (Cofin 2003 and FIRB 2001, N°. RBNF01KJHT) and by the European Community (grant no. QLG2-CT-2001-01903).

References

[1] J.M. Maris, K.K. Matthay, J. Clin. Oncol. 17 (1999) 2264.
[2] D. Niethammer, R. Handgretinger, Eur. J. Cancer 31A (1995) 568.
[3] R. Ladenstein, T. Philip, C. Lasset, O. Hartmann, A. Garaventa, R. Pinkerton, J. Michon, J. Pritchard, T. Klingebiel, B. Kremens, A. Pearson, C. Coze, P. Paolucci, D. Frappaz, H. Gadner, F. Chauvin, J. Clin. Oncol. 16 (1998) 953.
[4] P.G. Righetti, A. Stoyanov, M. Zhukov, The Proteome Revisited: Theory and Practice of All Relevant Electrophoretic Steps, Elsevier Press, Amsterdam, 2001.
[5] L.A. Greene, W. Shain, A. Chalazonitis, X. Breakfield, J. Minna, H.G. Coon, M. Nirenberg, Proc. Natl. Acad. Sci. U.S.A. 72 (1975) 4923.
[6] B. Herbert, M. Galvani, M. Hamdan, E. Olivieri, J. McCarthy, S. Pedersen, P.G. Righetti, Electrophoresis 22 (2001) 2046.
[7] P.G. Righetti, Immobilized pH Gradients: Theory and Methodology, Elsevier Press, Amsterdam, 1990.
[8] H. Hamdan, P.G. Righetti, Mass Spectrom. Rev. 21 (2002) 287.
[9] F. Pastorino, C. Brignole, D. Marimpietri, P. Sapra, E.H. Moase, T.M. Allen, M. Ponzoni, Cancer Res. 63 (2003) 86.
[10] L. Raffaghello, G. Pagnan, F. Pastorino, E. Cosimo, C. Brignole, D. Marimpietri, P.G. Montaldo, C. Gambini, T.M. Allen, E. Bogenmann, M. Ponzoni, Int. J. Cancer 104 (2003) 559.
[11] A.F. Chambers, A.C. Groom, I.C. MacDonald, Nat. Rev. Cancer 2 (2002) 563.
[12] M. Stromstedt, M.R. Waterman, Biochim. Biophys. Acta 1261 (1995) 126.
[13] W.F. Patton, BioTechniques 28 (2000) 944.
[14] F. Antonucci, M. Chilosi, M. Santacatterina, B. Herbert, P.G. Righetti, Electrophoresis 23 (2002) 356.
[15] F. Antonucci, M. Chilosi, C. Parolini, M. Hamdan, H. Astner, P.G. Righetti, Electrophoresis 24 (2003) 2376.
[16] D. Cecconi, A. Scarpa, M. Donadelli, M. Palmieri, M. Hamdan, H. Astner, P.G. Righetti, Electrophoresis 24 (2003) 1871.
[17] E. Colombo, J.C. Marine, D. Danovi, B. Falini, P.G. Pelicci, Nat. Cell Biol. 4 (2002) 529.
[18] M. Okuda, Oncogene 21 (2002) 6170.
[19] C. Yang, D.A. Maiguel, F. Carrier, Nucleic Acid Res. 30 (2002) 2251.
[20] G.M. Shackleford, A. Ganguly, C.A. MacArthur, BMC Genomics 2 (2001) 8.
[21] D. Bischof, K. Pulford, D.Y. Mason, S.W. Morris, Mol. Cell. Biol. 17 (1997) 2312.
[22] E. Alli, J. Vash-Babula, J.M. Yang, W.N. Hait, Cancer Res. 62 (2002) 6864.
[23] C.L. Chang, N. Hora, N. Huberman, R. Hinderer, M. Kukuruga, S.M. Hanash, Proteomics 1 (2001) 1415.
[24] G. Chen, H. Wang, T.G. Gharib, C.C. Huang, D.G. Thomas, K.A. Shedden, R. Kuick, J.M. Taylor, S.L. Kardia, D.E. Misek, T.J. Giordano, M.D. Iannettoni, M.B. Orringer, S.M. Hanash, D.G. Beer, Mol. Cell Proteomics 2 (2003) 107.
[25] N. Melhem, N. Hailat, R. Kuick, S.M. Hanash, Leukemia 11 (1997) 1690.